Available online at www.sciencedirect.com

SCIENCE DIRECT®

Chemical Physics Letters 421 (2006) 281–286

CHEMICAL PHYSICS LETTERS

www.elsevier.com/locate/cplett

The Rh–ligand bond: RhX (X = C, N, O, F, P and Cl) molecules

F. Stevens [a,b], V. Van Speybroeck [b], I. Carmichael [c], F. Callens [a], M. Waroquier [b,*]

[a] *Department of Solid State Sciences, Ghent University, Krijgslaan 281-S1, B-9000 Ghent, Belgium*
[b] *Center for Molecular Modeling, Laboratory of Theoretical Physics, Ghent University, Proeftuinstraat 86, B-9000 Ghent, Belgium*
[c] *Radiation Laboratory, University of Notre Dame, Notre Dame, IN 46556, USA*

Received 27 October 2005; in final form 9 December 2005
Available online 20 February 2006

Abstract

Bond distances, vibrational frequencies and dipole moments of the RhX (X = C, N, O, F, P and Cl) molecules were studied by density functional theory (DFT) methods. For all molecules under consideration, spectroscopic properties are computed using various functionals. This study is the first systematic ab initio investigation of the RhX molecules and in those cases where comparison with experimental data can be made, good quantitative agreement is achieved when using the BP86 functional.

1. Introduction

The chemistry of rhodium is very important in surface science and for catalytic applications since the metal can easily coordinate with many organic and inorganic molecules, which are in turn very reactive and widely used for fundamental investigations on catalysis in both laboratory and industry [1,2]. End of the 1960s RhC spectra have already been measured [3,4] in the gas phase, but it is only since a few years that extensive experimental studies on the whole series of the Rh–X (X = C, N, O, F, P and Cl) diatomic molecules have been performed [5–11].

The first theoretical work concerning these molecules dates from the early 1980s [12–14], in which RhC and RhN were investigated using configuration interaction (CI) methods. Recently, the performance of density functional theory (DFT) on transition metal (TM) dimers [15] and TM–ligand molecules [16,17] has been investigated. The latter studies showed that DFT methods are suited to describe high spin TM molecules. The application of DFT methods might be interesting for these systems since they can also be used for larger systems due to their low computational cost.

In this work, we report a DFT study on the ground state of the RhX molecules. For the tested molecules, the equilibrium bond length (r_e), harmonic vibrational frequency (ω_e) and the dipole moment (μ) were calculated. For those molecules for which DFT gives a less accurate description, multiconfigurational self-consistent field calculations within the complete active space (CASSCF) were performed to estimate the configurational composition of the predicted ground state. The motivation lies in the work of Li et al. [11], who stated that the recent experimental results on RhP might be a stimulus for ab initio predictions on the RhP molecule and related Rh–P systems of greater complexity. The principal aim of the present work is the development of a computational scheme for the accurate description of the phosphor–TM bond.

2. Computational details

Five exchange-correlation forms are tested which can be grouped in the following classes: (i) local density approximation: Stoll VWN [18,19]; (ii) general gradient approximation (GGA): BP86 [20,21]; (iii) meta-GGA: meta-BP86 [22]; (iv) special class of functionals which have the correct asymptotic behavior: Lb94 [23] and (v) hybrid functionals:

---

[*] Corresponding author.
E-mail addresses: franky.stevens@ugent.be (F. Stevens), michel.waroquier@ugent.be (M. Waroquier).

0009-2614/$ - see front matter © 2006 Elsevier B.V. All rights reserved.
doi:10.1016/j.cplett.2006.01.102

B3LYP [24]. The present DFT calculations are performed using the AMSTERDAM DENSITY FUNCTIONAL (ADF) program package [25,26], version 2004, and the GAUSSIAN2003 (G03) program package [27].

Exchange correlation forms which belong to the first four classes are studied using the ADF program package using the following full electron zero order regular approximation (ZORA) basis sets: single-ζ (SZ), double-ζ (DZ), double-ζ with polarization function (DZP), triple-ζ with polarization function (TZP), triple-ζ with two polarization functions (TZ2P) and a quadrupole-ζ with four polarization functions (QZ4P).

The G03 program package is employed when performing calculations with hybrid functionals (B3LYP), in combination with the full electron 3-21G [28] basis set and the pseudopotential basis LanL2DZ [29,30].

As the BP86 functional form is implemented in both G03 and ADF packages this functional has been chosen for a full investigation of the basis set dependence of the spectroscopic data.

Prior to calculating a spectroscopic property, the geometry of the molecule under consideration is optimized at that level of theory. For some functionals (meta-GGA and special functionals), analytic geometry optimizations are not possible. In these cases, a pointwise scan was performed when varying the internuclear distance in order to obtain the configuration which is lowest in energy. Also, when using special functionals (Lb94), the computation of the vibrational frequency is not possible in ADF and is therefore not reported.

Multiconfigurational self-consistent field calculations within the complete active space (CASSCF) method employing the DALTON suite of electronic structure programs [31] are used to estimate the configurational composition of the predicted electronic ground states. These calculations were performed with the 3-21G basis set correlating the ns and np electrons on the main group element and the outer ns and n-1d shells on the transition metal atom. The 3-21G basis set is of split-valence quality comprising [3s2p] on C, N, O and F, [4s3p] on P and Cl, and [6s5p4d] on Rh contractions of larger primitive GAUSSIAN sets.

3. Computational results

Phosphorus on its own is challenging for ab initio methods [32]. Therefore, we first investigate the Rh–ligand bond with carbon as connecting atom, which is easier to treat than phosphorus. The most suitable level of theory is then further applied to the RhC → RhF molecules. Finally the RhP molecule is investigated and compared to results for the RhCl molecule, which has a ligand from the same series of the periodic table and to RhN, which is iso-electronic to RhP.

3.1. Case study: RhC

3.1.1. Determination of the ground state

The present DFT calculations with ADF, using the BP86 functional, predict the paramagnetic ground state to be $^2\Sigma^+$ (Table 1), which is confirmed by experimental results [5]. The inclusion of scalar relativistic (SR) effects changes the energy difference between the various electronic states by ≈0.1 eV, compared to the not relativistic (NR) results (Table 1, first three columns). Nevertheless, the calculated ground state in both cases is in agreement with the known experimental ground state. When other functionals are applied, similar conclusions can be made.

3.1.2. Influence of SR effects on spectroscopic data

In Table 2, the computed spectroscopic data for the RhC molecule, using a NR and SR approach, are compared. Additionally, the percental deviation from the experimental values is given. The effect of relativistic effects on the dipole moment may amount to 0.3 Debye but is also strongly dependent on the applied functional. The inclusion of SR effects tends to shorten the bond length, shifting

Table 2
Comparison of computed spectroscopic parameters for RhC using a non-relativistic (NR) and scalar-relativistic (SR) approach. Basis set QZ4P is systematically used for all values. Additionally, the percental deviation from the experimental data is given

	Spectroscopic data			% Deviation	
	μ (D)	r_e (Å)	ω_e (cm^{-1})	r_e	ω_e
Experiment[a]	n.a.	1.613	1049.9		
SVWN(NR)	1.227	1.617	1057.7	0.2	0.7
BP86(NR)	1.474	1.632	1082.4	1.2	3.1
meta-BP86(NR)	1.427	1.620	1102.4	0.4	5.0
Lb94(NR)	1.322	1.608	n.a.	−0.3	n.a.
SVWN(SR)	1.399	1.606	1109.7	−0.4	5.7
BP86(SR)	1.746	1.619	1079.6	0.4	2.8
meta-BP86(SR)	1.691	1.612	1098.7	−0.1	4.6
Lb94(SR)	1.504	1.600	n.a.	−0.8	n.a.

[a] Ref. [5].

Table 1
Determination of the ground state configuration of the RhX (X = C, N, O, F, P and Cl) molecules. For each molecule, the experimental ground state (GS) configuration is given. All binding energies are referred to the most stable configuration of the molecule. The calculations were performed using the BP86 functional in combination with a QZ4P basis set and scalar relativistic (SR) corrections were considered, unless otherwise stated (NR)

	RhC(SR)	RhC(NR)	RhO		RhN	RhF	RhP(SR)	RhP(NR)	RhCl
$^2\Sigma^+$	0.000	0.000	0.297	$^1\Sigma^+$	0.000	0.641	0.000	0.191	1.991
$^4\Sigma^-$	2.256	2.317	0.000	$^3\Pi$	1.478	0.000	0.104	0.000	0.000
$^6\Sigma^-$	4.621	4.538	2.266	$^5\Delta$	3.894	1.300	0.657	0.603	1.331
Experimental GS	$^2\Sigma^+$	$^2\Sigma^+$	$^4\Sigma^-$		$^1\Sigma^+$	$^3\Pi$	$^1\Sigma^+$	$^1\Sigma^+$	$^3\Pi$

it closer to the experimental value for the BP86 functional. Large variations are observed for the computed vibrational frequency in case of the SVWN functional, while for the other functionals the influence of SR effects is much smaller. Nevertheless, the experimental vibrational frequency is nicely reproduced in all cases (NR and SR). Summarizing, the NR and SR predictions are of the same quantitative level, but we give preference to the SR option in ADF in all further calculations. The use of the LanL2DZ basis set in G03 automatically involves relativistic effects.

3.1.3. Basis set effects

When increasing the basis set size from SZ to QZ4P, convergence in the computed vibrational frequency and internuclear distance for RhC is found (Fig. 1, Table 3). Although the QZ4P value for the vibrational frequency slightly overestimates the experiment, the percental deviation is small (≈3%). The computed dipole moment is more dependent on the applied basis set on the other hand and no systematic convergence is noticed. As no experimental data are available on this quantity, the performance is more difficult to quantify. In view of the previous results, the QZ4P basis is further used in all ADF calculations.

Only a limited number of GAUSSIAN basis sets are available for Rh in the G03 program package and only results for a 3-21G and LanL2DZ basis set are reported in Fig. 1 and Table 3. The pseudopotential-based LanL2DZ basis (including relativistic effects) and the 3-21G basis set give comparable accuracy and they perform particularly well for describing the vibrational frequency. The former basis set is mostly applied in the literature and is therefore used in all further G03 calculations.

3.1.4. Influence of functional form

In Table 4, computed spectroscopic data for RhC, using 5 different functional forms, are listed. They all succeed in reproducing the two experimental data available in RhC, but the reference material is too restricted for making a conclusive choice as most efficient functional. In particular the BP86 functional performs well. A similar conclusion was made in the investigation of Z–ligand (Z = Cr, Mo, W) molecules [17].

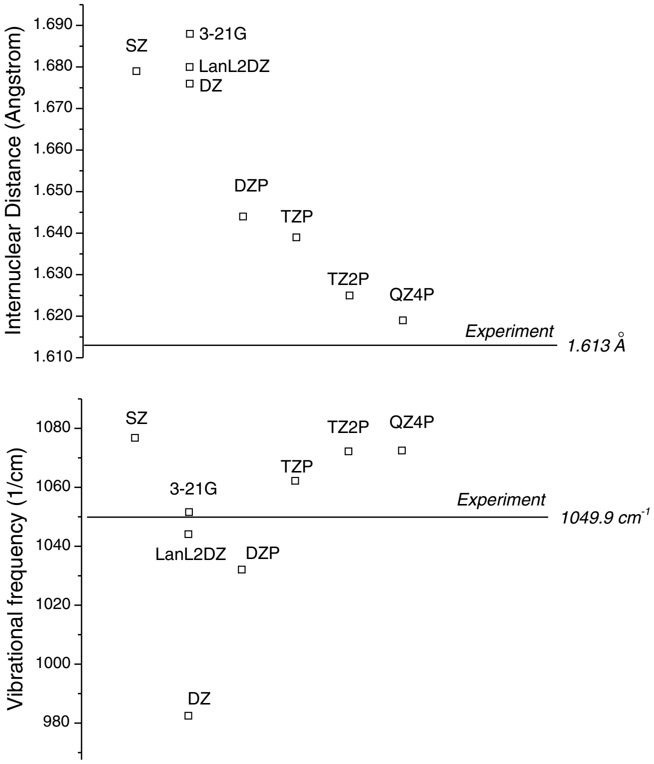

Fig. 1. Computed spectroscopic data for the RhC molecule as a function of the applied basis set using the BP86 functional.

3.1.5. Magnetic resonance data

For the RhC molecule, which is paramagnetic, also electron paramagnetic resonance (EPR) [33] data are available [4]. The main quantities determined in an EPR experiment are the *g* and hyperfine tensors, which describe the interaction between (i) the electron spin and the external magnetic field and (ii) a nuclear spin and the electron spin,

Table 3
Influence of basis set effects, using the BP86 functional, on the computed spectroscopic data of the RhC and RhP molecules using both the ADF and the G03 program package. In comparison, the percental deviation from the experimental data is given

Program package	Basis set	RhC molecule					RhP molecule				
		Spectroscopic data			% Deviation		Spectroscopic data			% Deviation	
		μ	r_e	ω_e	r_e	ω_e	μ	r_e	ω_e	r_e	ω_e
	Experiment	n.a.	1.613[a]	1049.9[a]			n.a.	1.86[b]	512.2[b]		
ADF	SZ	0.593	1.679	1076.8	4.1	2.6	2.279	2.049	604.7	10.2	18.1
	DZ	1.681	1.676	982.5	3.9	−6.4	0.559	2.093	522.8	12.5	2.1
	DZP	1.537	1.644	1032.1	1.9	−1.7	0.269	2.015	545.2	8.3	6.4
	TZP	1.660	1.639	1062.2	1.6	1.2	0.728	2.011	524.8	8.1	2.5
	TZ2P	1.579	1.625	1072.2	0.8	2.1	0.658	1.994	524.3	7.2	2.4
	QZ4P	1.746	1.619	1079.6	0.4	2.8	0.729	1.987	525.2	6.8	2.5
G03	3-21G	1.454	1.688	1051.6	4.7	0.2	0.261	2.074	533.2	11.5	4.1
	LanL2DZ	1.754	1.680	1044.1	4.1	−0.6	1.101	2.086	521.7	12.2	1.9

[a] Ref. [5].
[b] Ref. [11].

Table 4
Overview of the computational results using five different classes of functionals. For all molecules, the dipole moment, internuclear distance and vibrational frequency are given. All calculations have been performed with ADF, using the QZ4P basis set, except for the B3LYP functional, where use is made of G03 (with the LanL2DZ basis set)

	XC	RhC	RhN	RhO	RhF	RhP	RhCl
μ (Debye)	SVWN	1.399	3.267	3.041	3.428	0.373	3.159
μ (Debye)	BP86	1.746	3.372	3.235	4.061	0.729	3.635
μ (Debye)	meta-BP86	1.691	1.486	3.092	3.660	0.621	3.971
μ (Debye)	B3LYP	1.929	2.466	4.107	4.981	1.051	4.350
μ (Debye)	Lb94	1.504	1.560	3.132	3.441	0.515	3.380
μ (Debye)	Experiment	n.a.	n.a.	n.a.	n.a.	n.a.	n.a.
r_e (Å)	SVWN	1.606	1.611	1.693	1.867	1.969	2.161
r_e (Å)	BP86	1.619	1.632	1.709	1.900	1.987	2.228
r_e (Å)	meta-BP86	1.612	1.611	1.725	1.891	1.985	2.215
r_e (Å)	B3LYP	1.670	1.673	1.771	1.957	2.076	2.335
r_e (Å)	Lb94	1.600	1.611	1.689	1.852	2.010	2.199
r_e (Å)	Experiment	1.613[a]	1.642[a]	1.716[a]	1.964[a]	1.86[b]	2.275[b]
ω_e (cm^{-1})	SVWN	1109.7	1091.8	876.8	637.3	545.2	418.1
ω_e (cm^{-1})	BP86	1079.6	1042.4	846.9	548.5	525.2	317.0
ω_e (cm^{-1})	meta-BP86	1098.7	1012.2	819.1	569.5	564.5	322.9
ω_e (cm^{-1})	B3LYP	1057.6	987.4	809.8	531.5	530.1	323.2
ω_e (cm^{-1})	Experiment	1049.9[c]	894.9[d]	805.0[e]	575.0[a]	512.2[b]	≈340[b]

[a] Ref. [10].
[b] Ref. [11].
[c] Ref. [5].
[d] Ref. [6].
[e] Ref. [8].

Table 5
Influence of the applied functional form on the calculated EPR (hyperfine (in MHz) and g) values for the RhC molecule

	Experiment[a]	SVWN	BP86	meta-BP86	Lb94	B3LYP
$g_{\perp}$	2.0541	2.0504	2.0528	2.0538	2.0524	2.0839
$g_{\parallel}$	2.0039	2.0005	2.0032	2.0031	2.0003	2.0036
$A_{\perp}(^{103}\text{Rh})$	−1089	−1034.4	−1048.6	−1037.2	−1061.1	n.a.
$A_{\parallel}(^{103}\text{Rh})$	−1113	−1041.9	−1056.9	−1045.7	−1069.1	n.a.
$A_{iso}(^{103}\text{Rh})$	−1097	−1036.9	−1051.4	−1040.1	−1063.8	n.a.
$A_{\perp}(^{13}\text{C})$	55	75.4	61.8	64.8	73.3	n.a.
$A_{\parallel}(^{13}\text{C})$	89	102.1	89.6	92.1	101.2	n.a.
$A_{iso}(^{13}\text{C})$	66.3	84.3	71	73.9	82.6	n.a.

[a] Ref. [4].

respectively. All computed EPR parameters are taken up in Table 5.

In the discussion of the g tensor it was observed experimentally that $g_{\perp} > g_{\parallel}$, which is correctly reproduced computationally by all functionals. On the contrary, the SVWN and Lb94 functional forms predict the $g_{\parallel}$ smaller than the free electron value $g_{\parallel} < g_e$, in contrast with experiment. The relative deviations of the g factors with respect to the free electron value form a stringent test to validate the functional. In this context the (meta-)BP86 functional turns out to give the best overall agreement with the experimental data.

The theoretically predicted hyperfine values are in qualitative agreement with the experimental data (Table 5): (i) $|A_{\perp}| < |A_{\parallel}|$, with $|A_{\parallel}|$ along the Rh–X axis, for both ^{103}Rh and ^{13}C and (ii) $|A_{iso}(^{103}\text{Rh})| \gg |A_{iso}(^{13}\text{C})|$. Qualitatively, the agreement between computed and experimental data is good, although the anisotropy of the hyperfine couplings ($A_{\perp}$–$A_{\parallel}$) is somewhat underestimated by the calculations. Both experiment and theory give negative ^{103}Rh hyperfine values, which is a consequence of $g_n(^{103}\text{Rh}) < 0$.

The Rh hyperfine couplings are not able to discriminate between the various functionals. On the contrary, the carbon couplings show a slight preference to the BP86 functional yielding also a good quantitative agreement while most of the other functionals are only able to predict the correct anisotropy of the hyperfine couplings.

3.2. Further validation: RhN, RhO and RhF

In this section, we focus on the overall performance of DFT on the whole series of RhC → RhF molecules. For these molecules, the computed electronic configuration which is lowest in energy agrees with the experimental observations (Table 1). The best agreement with the experimental internuclear distance is obtained when the BP86 functional is used (Table 4). For the vibrational frequencies, the B3LYP functional gives the best agreement with experiment for the RhC, RhN and RhO molecules, although all functionals give results in the close vicinity of experiment. It is commonly known for standard organic applications that this hybrid functional gives good predictions of the harmonic frequencies [34].

3.3. Previous computational results: configuration interaction vs. DFT

In Table 6, experimental data for RhC and RhN are compared with the present DFT results (using the BP86/QZ4P level of theory) and previous CI results. As compared to the CI results, the quantitative agreement between predicted and experimental spectroscopic data using DFT techniques is much better for the RhC molecule. In case of the RhN molecule on the other hand, CI techniques give somewhat better agreement. The predicted DFT value of 3.372 Debye for the dipole moment is larger than the value of 2.08 Debye obtained using CI techniques. Nevertheless, no final conclusion concerning this property can be made due to the lack of experimental results.

3.4. The rhodium–phosphor bond: RhP

The previous results suggest that DFT can be successfully applied for the description of RhX molecules, with X an element of the first row of the periodic table. Nevertheless, it is not clear if a similar description is valid for ligands that belong to the second row of the periodic table. Therefore, a more elaborated discussion is given on RhP and cross reference is made with RhCl and RhN.

A first indication that the RhP molecule should be treated with great care is the strong influence of SR effects on the ground state configuration. As is clear from the data listed in Table 1, the $^3\Pi$ ground state is predicted when no relativistic corrections are included, while the $^1\Sigma^+$ ground state is obtained when SR effects are considered. The latter case is in agreement with experiment. The underlying reason is related to the small energy difference between the $^3\Pi$–$^1\Sigma^+$ states (≈0.1 eV), which is now of the order of the energy change when SR effects are included (see above).

Relatively small variations in the percental deviations are noticed when increasing the basis set size, starting from a TZP basis set (Table 3). The QZ4P basis gives the best overall agreement with experimental data. When the G03 program package is applied, a LanL2DZ basis is preferred.

All functionals overestimate the internuclear distance of the RhP molecule. The best performing functionals are (meta-)BP86 and SVWN (Table 4).

For RhCl, the agreement with the experimental internuclear distance is much better.

Summarizing, if also the reproduction of the experimental vibrational frequencies of both RhP and RhCl is taken into consideration, the best overall quantitative agreement is again achieved by the BP86 functional.

The underlaying physical reason for the less accurate description of the internuclear distance of the RhP molecule is probably related to the single configuration character of DFT. As can be concluded from the CASSCF results for the RhP molecule (Table 7), the dominant $^1\Sigma^+$ configuration has a weight of only 54% and there should be many configurations with small, but significant, contributions. Nevertheless, the CASSCF internuclear distance of 2.3 Å is significantly larger then the experimental value and the experimental vibrational frequency is seriously underestimated. Based on the weight of the dominant $^1\Sigma^+$ configuration of the iso-electronic RhN molecule (74%), which has the same ground state as the RhP molecule, better DFT results are expected, as is indeed observed.

Table 7
CASSCF results for the iso-electronic RhN and RhP molecules using a 3-21G basis set. For each molecule, the weight of the dominant configuration is given and comparison with experimental spectroscopic data is made

	RhN		RhP	
	Experiment[a]	CASSCF	Experiment[b]	CASSCF
Ground state	$^1\Sigma^+$	$^1\Sigma^+$	$^1\Sigma^+$	$^1\Sigma^+$
Weight	n.a.	74%	n.a.	54%
r_e (Å)	1.642	1.794	1.86	2.315
ω_e (cm^{-1})	894.9	662	512.2	209

[a] Ref. [6].
[b] Ref. [11].

Table 6
Comparison between experimental and DFT (using the BP86 functional in combination with a QZ4P basis set) and previous configuration interaction (CI) results

	RhC				RhN		
	Experiment[a]	DFT	CI[b]	FOCI[c]	Experiment[d]	DFT	MCSCF CISD[e]
μ (Debye)	n.a.	1.746	n.a.	n.a.	n.a.	3.372	2.08
r_e (Å)	1.613	1.619	1.715	1.575	1.642	1.632	1.640
ω_e (cm^{-1})	1049.9	1079.6	821	1102	894.9	1042.4	846

[a] Ref. [5].
[b] Ref. [12].
[c] Ref. [14].
[d] Ref. [6].
[e] Ref. [13].

Although one could suggest that DFT methods are less suited for the description of the RhP molecule due to the single configuration character of DFT, some further remarks need to be made. When increasing the atomic number of the ligand (RhC → RhCl, Table 4), the calculations predict a systematic increase in internuclear distance and decrease in vibrational frequency, as could be expected intuitively. The latter dependency of the vibrational frequency is also noticed for the experimental values. The only exception to the systematic increase of the experimental internuclear distance is the RhP molecule. Further experimental attention should be given to this item to resolve this discrepancy.

4. Conclusion

In this work, the performance of DFT methods for the description of RhX di-atomic molecules is investigated. For all molecules under consideration, the experimental ground state was reproduced and the agreement with the available experimental spectroscopic and magnetic resonance date was good. The theoretical results, presented in this work, give a good indication that DFT could be a viable method to describe the TM–ligand bond in more complex molecules. In case of the RhP molecule, somewhat worse quantitative agreement between the computed and experimental internuclear distance was obtained. Based on CASSCF results, it was shown that this molecule has a multiconfiguration character and should be treated with great care when performing DFT calculations.

Acknowledgments

The authors thank the Fund for Scientific Research (FWO-Flanders, Belgium) for financial support. The Notre Dame Radiation Laboratory is supported by the Office of Basic Energy Sciences of the United States Department of Energy.

References

[1] H.J. Miessner, J. Am. Chem. Soc. 116 (1994) 11522.
[2] E.A. Wovchko, J.T. Yates, J. Am. Chem. Soc. 118 (1996) 10250.
[3] A. Lagerqvist, R. Scullman, Ark. Fys. 32 (1966) 479;
B. Kaving, R. Scullman, J. Mol. Spectrosc. 32 (1969) 475.
[4] J.M. Brom, W.R.M. Graham, W. Weltner, J. Chem. Phys. 57 (1972) 4116.
[5] W.J. Balfour, S.G. Fougre, R.F. Heuff, C.X.W. Qian, C. Zhou, J. Mol. Spectrosc. 198 (1999) 393.
[6] S.G. Fougre, W.J. Balfour, J. Cao, C.X.W. Qian, J. Mol. Spectrosc. 199 (2000) 18.
[7] R.F. Heuff, W.J. Balfour, A.G. Adam, J. Mol. Spectrosc. 216 (2002) 136.
[8] R.H. Jensen, S.G. Fougre, W.J. Balfour, Chem. Phys. Lett. 370 (2003) 106.
[9] R.F. Heuff, S.G. Fougere, W.J. Balfour, J. Mol. Spectrosc. 231 (2005) 99.
[10] R. Li, R.H. Jensen, W.J. Balfour, S.A. Shepard, A.G. Adam, J. Chem. Phys. 121 (2004) 2591.
[11] R. Li, W.J. Balfour, J. Phys. Chem. A 108 (2004) 8145.
[12] I. Shim, K.A. Gingerich, J. Chem. Phys. 81 (1984) 5937.
[13] I. Shim, K. Mandix, K.A. Gingerich, J. Mol. Struct. – Theochem. 393 (1997) 127.
[14] H. Tan, M. Liao, K. Balasubramanian, Chem. Phys. Lett. 280 (1997) 423.
[15] N.E. Schultz, Y. Zhao, D.G. Truhlar, J. Phys. Chem. A 109 (2005) 4388.
[16] A. Citra, L. Andrews, J. Phys. Chem. A 103 (1999) 3410.
[17] F. Stevens, I. Carmichael, F. Callens, M. Waroquier, J. Phys. Chem. A (in press).
[18] S.H. Vosko, L. Wilk, M. Nusair, Can. J. Phys. 58 (1980) 1200.
[19] H. Stoll, C.M.E. Pavlidou, H. Preuss, Theor. Chim. Acta 49 (1978) 143.
[20] J.P. Perdew, Phys. Rev. B 33 (1986) 8822.
[21] A.D. Becke, Phys. Rev. A 38 (1988) 3098.
[22] E.I. Proynov, S. Sirois, D.R. Salahub, Int. J. Quantum Chem. 64 (1997) 427.
[23] R. van Leeuwen, E.J. Baerends, Phys. Rev. A 49 (1994) 2421.
[24] A.D. Becke, J. Chem. Phys. 98 (1993) 5648.
[25] C.F. Guerra, J.G. Snijders, G.T. te Velde, E.J. Baerends, Theor. Chem. Acc. 99 (1998) 391.
[26] G.T. te Velde, F.M. Bickelhaupt, S.J.A. van Gisbergen, C. Fonseca, E.J. Baerends, J.G. Snijders, T. Ziegler, J. Comput. Chem. 22 (2001) 931.
[27] M.J. Frisch et al., GAUSSIAN 03, Revision A.1, Gaussian Inc., Pittsburgh, PA, 2003.
[28] K.D. Dobbs, W.J. Hehre, J. Comput. Chem. 8 (1987) 861.
[29] T.H. Dunning Jr., P.J. Hay, in: H.F. SchaeferIII (Ed.), Methods of Electronic Structure, Theory, vol. 2, Plenum Press, 1977.
[30] J.V. Ortiz, P.J. Hay, R.L. Martin, J. Am. Chem. Soc. 114 (1992) 2736.
[31] DALTON, A Molecular Electronic Structure Program, Release 2.0, 2005. Available from: <http://www.kjemi.uio.no/software/dalton/dalton.html>.
[32] T. Leyssens, D. Peeters, J. Mol. Struct. 686 (2004) 71.
[33] N.M. Atherton, Principals of Electron Spin Resonance, Prentice Hall, New York, 1993.
[34] R. Gomez-Balderas, M.L. Coote, D.J. Henry, L. Radom, J. Phys. Chem. A 108 (2004) 2874.